A Generalized Memory Polynomial Model for Digital Predistortion of RF Power Amplifiers

Dennis R. Morgan, *Senior Member, IEEE*, Zhengxiang Ma, Jaehyeong Kim, Michael G. Zierdt, and John Pastalan

***Abstract*—Conventional radio-frequency (RF) power amplifiers operating with wideband signals, such as wideband code-division multiple access (WCDMA) in the Universal Mobile Telecommunications System (UMTS) must be backed off considerably from their peak power level in order to control out-of-band spurious emissions, also known as "spectral regrowth." Adapting these amplifiers to wideband operation therefore entails larger size and higher cost than would otherwise be required for the same power output. An alternative solution, which is gaining widespread popularity, is to employ digital baseband predistortion ahead of the amplifier to compensate for the nonlinearity effects, hence allowing it to run closer to its maximum output power while maintaining low spectral regrowth. Recent improvements to the technique have included *memory* effects in the predistortion model, which are essential as the bandwidth increases. In this paper, we relate the general Volterra representation to the classical Wiener, Hammerstein, Wiener–Hammerstein, and parallel Wiener structures, and go on to describe some state-of-the-art predistortion models based on memory polynomials. We then propose a new generalized memory polynomial that achieves the best performance to date, as demonstrated herein with experimental results obtained from a testbed using an actual 30-W, 2-GHz power amplifier.**

***Index Terms*—Memory polynomial, power amplifiers, predistortion, spectral regrowth, Universal Mobile Telecommunications System (UMTS), wideband code-division multiple access (WCDMA).**

I. Introduction

CONVENTIONAL radio-frequency (RF) power amplifiers operating with wideband signals, such as wideband code division multiple access (WCDMA) used in the Universal Mobile Telecommunications System (UMTS), are particularly susceptible to the generation of out-of-band spurious emissions, also referred to as "spectral regrowth." Regulatory agencies mandate control of these emissions, and various techniques are available for this purpose. The most obvious solution is to back off the amplifier input level so as to keep well within the linear portion of the operating curve. However, this simple remedy carries the disadvantages of a larger size and higher cost than would otherwise be required to deliver the same output power. Feedforward, in which the distortion is subtracted out at the output, is another technique that has been employed for linearizing power amplifiers [1]. However, this also entails a considerable increase in cost because of the analog combining networks that must operate at output power levels and the need for an extra (lower power, but highly linear) RF amplifier. Another technique, known as *linear amplification with nonlinear components* (LINC) [1, sec. 7], combines the outputs of two phase-altered nonlinear power amplifiers to realize overall linear operation but still requires a high power analog combining network. An alternative solution, which is gaining widespread popularity, is to employ digital baseband predistortion ahead of the amplifier to compensate for the nonlinearity effects, hence allowing operation nearer to the maximum rated power while maintaining low spectral regrowth. The digital predistortion (DPD) solution has the potential for significantly reducing size and cost over that of other methods and may be an indispensable enabling technology for the widespread deployment of software defined radio and also new network topologies involving tower top RF electronics [2]. As a measure of effectiveness, it is estimated in [2] that conventional power amplifiers for WCDMA achieve efficiencies (ratio of output RF power to input dc power) in the range of 3%–5%, while feedforward increases this to 6%–8%. DPD, on the other hand, is currently able to achieve efficiencies of 8%–10%, and future projections are in excess of 15%.

Current DPD implementations mostly use *memoryless* techniques, by which is meant that the predistortion is an instantaneous nonlinearity that tries to compensate for the instantaneous nonlinear behavior of the power amplifier. This instantaneous behavior is characterized in terms of AM/AM and AM/PM effects, whereby both the amplitude and phase are functions of the instantaneous value of the input signal amplitude. Early predistortion techniques, exemplified by [3], were custom-tailored to specific digital modulation formats involving a relatively small alphabet of input states. Generalization of this technique using amplitude and phase lookup tables (LUTs) accommodates arbitrary input signals (see [4] and references therein), which is much more useful for general applications (see, e.g., [5] and references therein).

In order to fully exploit the potential of DPD, memory effects must be taken into account [6]–[8]. The causes of these effects include transport delay and rapid thermal time constants of the active devices themselves, as well as components in the biasing circuits that give rise to effects that are dependent on the signal envelope. These effects become more important as the bandwidth increases. Therefore, the generalization of memoryless DPD to memory structures is essential to realize the full potential of the technique in modern wideband applications.

Manuscript received December 29, 2004; revised November 7, 2005. The associate editor coordinating the review of this manuscript and approving it for publication was Prof. John J. Shynk.

D. R. Morgan, Z. Ma, M. G. Zierdt, and J. Pastalan are with Bell Laboratories, Lucent Technologies, Murray Hill, NJ 07974-0636 USA (e-mail: drrm@lucent.com; xiang@lucent.com; zeta@lucent.com jzp@lucent.com).

J. Kim was with the Wireless Advanced Technology Laboratory, Lucent Technologies. He is now with POSDATA, Ltd., Seongnam-city, Kyeonggi-do, Korea (e-mail: jaekim@posdata.co.kr).

Digital Object Identifier 10.1109/TSP.2006.879264

1053-587X/$20.00 © 2006 IEEE

Authorized licensed use limited to: Technion Israel Institute of Technology. Downloaded on November 09,2022 at 15:11:17 UTC from IEEE Xplore. Restrictions apply.

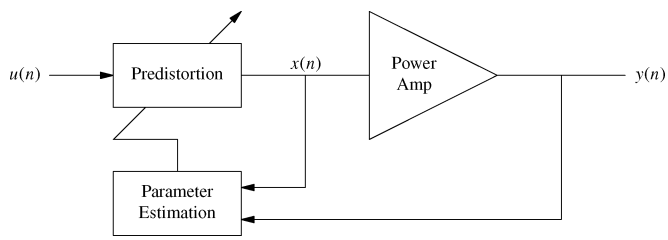

Fig. 1. Generic predistortion scheme.

In this paper, we focus on state-of-the-art memory models that are capable of wideband DPD. We first discuss general approaches using Volterra series methods and then go on to formulate some simple special cases, including Wiener, Hammerstein, Wiener–Hammerstein, and parallel Wiener structures. The so-called "memory polynomial" is interpreted as a special case of a generalized Hammerstein model and is further elaborated by combining with the Wiener model. A new wideband predistortion model, which we call a *generalized memory polynomial* (GMP), is then introduced that combines the memory polynomial with cross terms between the signal and lagging and/or leading exponentiated envelope terms. Inverse structures and estimation algorithms are then discussed for the predistortion application, and a complete DPD linearization technique is developed based on the GMP. As with all DPD approaches, the new technique enjoys inherent implementation/cost advantages over other linearization techniques, as previously discussed. In addition, it will be demonstrated the the new GMP/DPD technique achieves the best performance to date, as demonstrated herein with experimental results obtained from a testbed using an actual 30-W, 2-GHz power amplifier.

II. Memory Structures

Fig. 1 illustrates the generic DPD scheme where $u(n)$ is the input signal to the predistortion unit, whose output $x(n)$ feeds the power amplifier to produce output $y(n)$. The most general form of nonlinearity with M-tap memory is described by the Volterra series, which consists of a sum of multidimensional convolutions [9], which in discrete time can be written

$$y(n) = \sum_{k=1}^{K} y_k(n) \tag{1}$$

where

$$y_k(n) = \sum_{m_1=0}^{M-1} \cdots \sum_{m_k=0}^{M-1} h_k(m_1, \cdots, m_k) \prod_{l=1}^{k} x(n - m_l) \tag{2}$$

is the k-dimensional convolution of the input with Volterra kernel h_k. This is a generalization of a power series representation with a finite memory of length M.

It is useful to rewrite (2) in an alternative form by making a change to "diagonal" index variables [10]

$$n_l = m_{l+1} - m_1, l = 1, 2, \cdots, k-1. \tag{3}$$

Thus, (2) becomes

$$y_k(n) = \sum_{n_1=-M+1}^{M-1} \sum_{n_2=-M+1}^{M-1} \cdots \sum_{n_{k-1}=-M+1}^{M-1} g^{(k)}_{n_1,\cdots,n_{k-1}}(n) * \left[x(n) \prod_{l=1}^{k-1} x(n - n_l) \right] \tag{4}$$

where $*$ denotes [one-dimensional (1-D)] convolution and

$$g^{(k)}_{n_1,\cdots,n_{k-1}}(n) = h_k(n, n + n_1, \cdots, n + n_{k-1}) \tag{5}$$

is a linear filter determined from the Volterra kernel h_k. This shows that an arbitrary kth-order Volterra term can be expressed as a sum of linear filter outputs, where the input to each filter is a product of k differentially delayed input signals of the form

$$x(n) \prod_{l=1}^{k-1} x(n - n_l). \tag{6}$$

The number of terms in (4) can be greatly reduced [10] by eliminating redundancies associated with the various index permutations of (6) and assuming, without loss of generality [9], that the kernels are symmetric. However, for our purposes, (4) will be adequate, as we only intend to use it as a general guide to amplifier models.

The general theory of Volterra series can be further specialized for the case of signals whose bandwidth is small compared to the center frequency (even though the bandwidth may be large in absolute terms). In this case, we can express the real input signal $x(n)$ in terms of its complex baseband representation $\tilde{x}(n)$ as

$$x(n) = \mathrm{Re}\left\{ e^{j\omega_0 n} \tilde{x}(n) \right\} = \frac{e^{j\omega_0 n}\tilde{x}(n) + e^{-j\omega_0 n}\tilde{x}^*(n)}{2} \tag{7}$$

where $\omega_0 = 2\pi f_0$ and f_0 is the center frequency. Substituting (7) into (6) and dropping all factors of 2 leads to products of the form

$$\left[e^{j\omega_0 n}\tilde{x}(n) + e^{-j\omega_0 n}\tilde{x}^*(n) \right] \times \prod_{l=1}^{k-1} \left[e^{j\omega_0 n}\tilde{x}(n - n_l) + e^{-j\omega_0 n}\tilde{x}^*(n - n_l) \right]. \tag{8}$$

Usually, for such signals, we are only interested in frequency components close to f_0. We observe from (8) that the only way that products of this form can result in such frequency components is when k is odd and the number of $\tilde{x}$ terms differs from the number of $\tilde{x}^*$ terms by exactly one. For example, with $k = 3$, one such product is of the form

$$\mathrm{Re}\left\{ e^{j\omega_0 n}\tilde{x}(n)\tilde{x}(n - n_1)\tilde{x}^*(n - n_2) \right\}. \tag{9}$$

Thus, all third-order baseband products are expressible as one of the following (or their complex conjugates):

$$\begin{aligned} &\tilde{x}(n)\tilde{x}(n - n_1)\tilde{x}^*(n - n_2) \\ &\tilde{x}(n)\tilde{x}^*(n - n_1)\tilde{x}(n - n_2) \\ &\tilde{x}^*(n)\tilde{x}(n - n_1)\tilde{x}(n - n_2). \end{aligned} \tag{10}$$

Authorized licensed use limited to: Technion Israel Institute of Technology. Downloaded on November 09,2022 at 15:11:17 UTC from IEEE Xplore. Restrictions apply.

Likewise, all fifth-order baseband products are like the combinations

$$\begin{aligned}
&\tilde{x}(n)\tilde{x}(n-n_1)\tilde{x}(n-n_2)\tilde{x}^*(n-n_3)\tilde{x}^*(n-n_4)\\
&\tilde{x}(n)\tilde{x}(n-n_1)\tilde{x}^*(n-n_2)\tilde{x}(n-n_3)\tilde{x}^*(n-n_4)\\
&\tilde{x}(n)\tilde{x}^*(n-n_1)\tilde{x}(n-n_2)\tilde{x}(n-n_3)\tilde{x}^*(n-n_4)\\
&\tilde{x}^*(n)\tilde{x}(n-n_1)\tilde{x}(n-n_2)\tilde{x}(n-n_3)\tilde{x}^*(n-n_4)\\
&\tilde{x}(n)\tilde{x}(n-n_1)\tilde{x}^*(n-n_2)\tilde{x}^*(n-n_3)\tilde{x}(n-n_4)\\
&\tilde{x}(n)\tilde{x}^*(n-n_1)\tilde{x}(n-n_2)\tilde{x}^*(n-n_3)\tilde{x}(n-n_4)\\
&\tilde{x}^*(n)\tilde{x}(n-n_1)\tilde{x}(n-n_2)\tilde{x}^*(n-n_3)\tilde{x}(n-n_4)\\
&\tilde{x}(n)\tilde{x}^*(n-n_1)\tilde{x}^*(n-n_2)\tilde{x}(n-n_3)\tilde{x}(n-n_4)\\
&\tilde{x}^*(n)\tilde{x}(n-n_1)\tilde{x}^*(n-n_2)\tilde{x}(n-n_3)\tilde{x}(n-n_4)\\
&\tilde{x}^*(n)\tilde{x}^*(n-n_1)\tilde{x}(n-n_2)\tilde{x}(n-n_3)\tilde{x}(n-n_4)
\end{aligned} \tag{11}$$

and so on. This process is similar to the method of [10], except that only real quantities are considered there, whereas we write everything in terms of complex baseband signals. In either case, the narrowband representation significantly reduces the number of terms that we have to consider and guides the choice of model architecture. In some cases, just using the first line of (10) and (11) may yield satisfactory performance [11].

At this point, for ease of notation, we will drop the over-tildes with the understanding that all signals are complex baseband. We further assume that the sampling rate of the complex baseband signal is high enough so that all products up to Kth order are alias-free, i.e., $KB/f_{\rm s} \leq 1$, where B is the bandwidth and $f_{\rm s}$ is the sampling rate.

We now consider some simpler memory structures, which are all special cases of the general formulations (2) and (4). The first of these are classical and are only described in fullband Volterra form, whereas more advanced models, consisting of variations on memory polynomials, are specialized at the outset to narrowband representations, as these are the most relevant to our practical application.

A. Wiener

A special case of the general Volterra formulation is the *Wiener* model [Fig. 2(a)], which consists of a linear filter (h) followed by a memoryless nonlinerity and is equivalent to taking

$$h_k(m_1,\cdots,m_k) = a_k h(m_1)\cdots h(m_k), k=1,2,\ldots,\ K \tag{12}$$

in (2), where a_k are the polynomial coefficients of the nonlinearity. Thus, the Wiener model is written

$$y_{\rm W}(n) = \sum_{k=1}^{K} a_k \left[\sum_{m=0}^{M-1} h(m)x(n-m)\right]^k. \tag{13}$$

Note that for narrowband applications, each of the power terms in (13) has to be expanded in various combinations as exemplified by (10) and (11).

The Wiener model has been studied for predistortion of TWT transmitters [12], [13], as well as a more general means for nonlinear system identification [14], [15]. The Wiener model is one of the simplest ways to combine memory effects with nonlinearity. However, its effectiveness in modeling most power amplifiers is very limited. Furthermore, the Wiener model has one undesirable attribute in that the output (13) depends *nonlinearly* on the coefficients $h(m)$, making their estimation more troublesome than for models that are linear in the parameters.

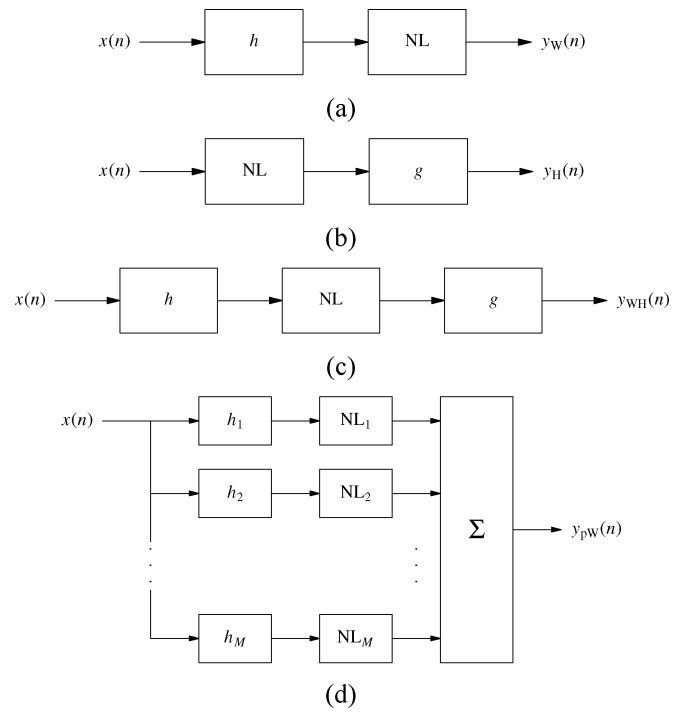

Fig. 2. Some common nonlinear memory models: (a) Wiener; (b) Hammerstein; (c) Wiener–Hammerstein; and (d) parallel Wiener.

B. Hammerstein

Another simple memory nonlinearity is the Hammerstein model [Fig. 2(b)], which is formed by a nonlinearity followed by a linear filter (g). In the alternative Volterra formulation (4), this corresponds to taking

$$g^{(k)}_{0,\cdots,0}(n) = a_k g(m),\ k=1,2,\ldots,K \tag{14}$$

with all other $g^{(k)}$'s set to zero. Thus, for the Hammerstein model, we have

$$y_{\rm H}(n) = \sum_{m=0}^{M-1} g(m) \sum_{k=1}^{K} a_k x^k(n-m). \tag{15}$$

Again, this is a very simple memory nonlinearity which has been studied for general applications [15] but is of limited effectiveness for predistortion. However, it does have the desirable property of being linear in the parameters $g(m)a_k$, i.e., if they are considered as a two-dimensional (2-D) array over m and k.

We observe that the Hammerstein and Wiener models can form mutual inverses if their linear filters have stable inverses and if their nonlinear polynomials are one-to-one inverses over the range of interest.

C. Wiener–Hammerstein

One can combine the Wiener and Hammerstein structures [Fig. 2(c)] to form a cascade consisting of a linear filter (h),

Authorized licensed use limited to: Technion Israel Institute of Technology. Downloaded on November 09,2022 at 15:11:17 UTC from IEEE Xplore. Restrictions apply.

memoryless nonlinearity, and another linear filter (g). Thus, the Wiener–Hammerstein model is written

$$y_{\mathrm{WH}}(n) = \sum_{m_2=0}^{M-1} g(m_2) \sum_{k=1}^{K} a_k \times \left[\sum_{m_1=0}^{M-1} h(m_1) x(n - m_1 - m_2) \right]^k . \quad (16)$$

The formal specification of this model in terms of the general Volterra model can be determined by first expressing the Wiener part [with kernel (12)] in the alternative Volterra form (4) and then convolving the resulting filters with the Hammerstein filter $g(n)$. Thus, (16) is equivalent to the alternative Volterra model (4) with filters

$$g^{(k)}_{n_1,\cdots,n_{k-1}}(n) = a_k g(n) * \left[h(n) h(n+n_1) \cdots h(n+n_{k-1}) \right], \quad k = 1, 2, \ldots, K. \quad (17)$$

The Wiener–Hammerstein model, although more general than either Wiener or Hammerstein model, is still nonlinear in the parameters $h(m_1)$. Nevertheless, it has been studied as a general analysis tool [16].

D. Memory Polynomial

One way to generalize the Hammerstein model is to choose different filters $g^{(k)}_{0,\cdots,0}(n)$ in (14) for each different order k. Thus, by combining the different filters and power series coefficients into a 2-D array $\{a_{km}\}$, we can formulate the generalized Hammerstein model as

$$y_{\mathrm{GH}}(n) = \sum_{k=1}^{K} \sum_{m=0}^{M-1} a_{km} x^k (n - m). \quad (18)$$

Now for the narrowband case, if we select only combinations of the form $x(n)|x(n-m)|^{k-1}$, we arrive at the model of Kim and Konstantinou [17], which we call a *memory polynomial* [18]

$$y_{\mathrm{MP}}(n) = \sum_{k=0}^{K-1} \sum_{m=0}^{M-1} a_{km} x(n-m) \left| x(n-m) \right|^k . \quad (19)$$

(Here and in the following, we use running index k to designate the *envelope* order.) The memory polynomial model has proven effective for predistortion of actual power amplifiers under typical operating conditions [17], [18]. We now go on to formulate more general memory structures that have the potential to achieve even better performance.

E. Parallel Wiener

The parallel Wiener model is formed by combining the outputs from several Wiener models [Fig. 2(d)] and has been suggested as a heuristic means for representing the behavior of a power amplifier at different envelope frequencies [19]. The parallel Wiener model can be fit into the general Volterra framework (1), (2) by simply adding the kernels of each subblock. An even more complicated model can be formed as a general Wiener model [20], whereby the nonlinear functions following the linear filters are all coupled as a multiple-input, single-output memoryless nonlinearity.

The parallel Wiener model can be seen as a generalization of the memory polynomial as follows. Suppose that we have M Wiener models indexed by $m = 1, 2, \cdots, M$, and let the linear filter for each be specified as a simple delay $h_m(n) = \delta(n-m)$. Now, if the nonlinearity for each Wiener model is specified as a polynomial with coefficients a_{km}, then we have exactly the memory polynomial of (19).

F. Memory-Polynomial/Wiener Model

The product terms in the memory polynomial (19) involve input samples at the same time instant, i.e., of the form $x^k(n - m)$. We know that the alternative general Volterra formulation (4) also involves products with *different* time shifts (6), which we will refer to as *cross terms*. One simple way to introduce memory cross terms is by way of the Wiener model (13). Starting with this form and following the example of (19), we collect the relevant narrowband cross terms as

$$\sum_{k=0}^{K-1} b_k x(n) \left[\sum_{m=0}^{M-1} c_m \left| x(n-m) \right| \right]^k \quad (20)$$

where b_k are the polynomial coefficients of the nonlinearity and c_m are the envelope filter coefficients. Combining this with the memory polynomial (19) defines the memory-polynomial/Wiener model [21].

$$y_{\mathrm{MPW}}(n) = \sum_{k=0}^{K-1} \sum_{m=0}^{M-1} a_{km} x(n-m) \left| x(n-m) \right|^k + \sum_{k=1}^{K-1} b_k x(n) \left[\sum_{m=0}^{M-1} c_m \left| x(n-m) \right| \right]^k . \quad (21)$$

(Note that the second term starts with envelope order $k = 1$ to avoid redundancy with the first term.)

In [22], a technique is presented for estimating the parameters of the memory-polynomial/Wiener model. The method alternately estimates a_{km} and b_k using least squares (for fixed c_m) and c_m using Newton's method (for fixed a_{km} and b_k). Because (21) is nonlinear in the c_m coefficients, convergence is somewhat unreliable and susceptible to getting trapped in local minima, being dependent on the initialization. Nevertheless, it does demonstrate a definite improvement over the memory polynomial model by virtue of the inclusion of cross terms.

G. Generalized Memory Polynomial

A more direct way to introduce cross terms is by means of the alternative Volterra formulation (4). Thus, a generalized form of the kth memory polynomial component in (19) is written

$$\sum_{k=0}^{K-1} \sum_{m=1}^{M} b_{km} x(n) \left| x(n-m) \right|^k \quad (22)$$

where we have inserted a delay of m samples between the signal and its exponentiated envelope. Taking multiple such delayed versions of (22) using both positive and negative cross-term

Authorized licensed use limited to: Technion Israel Institute of Technology. Downloaded on November 09,2022 at 15:11:17 UTC from IEEE Xplore. Restrictions apply.

time shifts and combining with (19) results in the generalized memory polynomial

$$\begin{aligned} y_{\mathrm{GMP}}(n) = &\sum_{k=0}^{K_a-1}\sum_{l=0}^{L_a-1} a_{kl}x(n-l)\left|x(n-l)\right|^k \\ &+\sum_{k=1}^{K_b}\sum_{l=0}^{L_b-1}\sum_{m=1}^{M_b} b_{klm}x(n-l)\left|x(n-l-m)\right|^k \\ &+\sum_{k=1}^{K_c}\sum_{l=0}^{L_c-1}\sum_{m=1}^{M_c} c_{klm}x(n-l)\left|x(n-l+m)\right|^k. \end{aligned} \tag{23}$$

(We recently became aware of a similar formulation in [23].) Here, K_aL_a are the number of coefficients for aligned signal and envelope (memory polynomial); $K_bL_bM_b$ are the number of coefficients for signal and lagging envelope; and, $K_cL_cM_c$ are the number of coefficients for signal and leading envelope. The advantage of this cross-term model is that the coefficients, like those of the memory polynomial, appear in *linear* form. Therefore, all of the coefficients can be simply and robustly estimated using any least-squares type of algorithm. This has favorable implications for algorithm stability and computational complexity.

In many cases, we do not require all of the coefficients in (23). For example, odd-order nonlinearities usually dominate so that we may only want to consider even-order envelope powers k, especially for the lagging and leading envelope terms (b_{klm} and c_{klm}). In addition, in some cases, depending on the signal bandwidth and sampling rate, it may not be necessary to implement all delay taps (l) over a given delay range. Therefore, in general, it is useful to rewrite (23) in terms of index arrays

$$\begin{aligned} y_{\mathrm{GMP}}(n) = &\sum_{k\in\mathcal{K}_a}\sum_{l\in\mathcal{L}_a} a_{kl}x(n-l)\left|x(n-l)\right|^k \\ &+\sum_{k\in\mathcal{K}_b}\sum_{l\in\mathcal{L}_b}\sum_{m\in\mathcal{M}_b} b_{klm}x(n-l)\left|x(n-l-m)\right|^k \\ &+\sum_{k\in\mathcal{K}_c}\sum_{l\in\mathcal{L}_c}\sum_{m\in\mathcal{M}_c} c_{klm}x(n-l)\left|x(n-l+m)\right|^k. \end{aligned} \tag{24}$$

Here, $\mathcal{K}_a$ and $\mathcal{L}_a$ are the index arrays for aligned signal and envelope; $\mathcal{K}_b$, $\mathcal{L}_b$, and $\mathcal{M}_b$ are the index arrays for signal and lagging envelope; and, $\mathcal{K}_c$, $\mathcal{L}_c$, and $\mathcal{M}_c$ are index arrays for signal and leading envelope.

H. Performance/Computational-Complexity

As we progress from the simple classical models to the more advanced variations of memory polynomials, the effectiveness of predistortion, in terms of reducing spectral regrowth, generally increases. However, there is an attending increase in computational complexity and this has to be weighed against other simpler expediencies, such as using a larger amplifier with increased backoff. Even for any particular scheme, performance will generally improve as the number of coefficients in the predistortion model is increased, at least up to some practical limit where a point of diminishing returns is reached. Some examples of the latter will be given later in the experimental section.

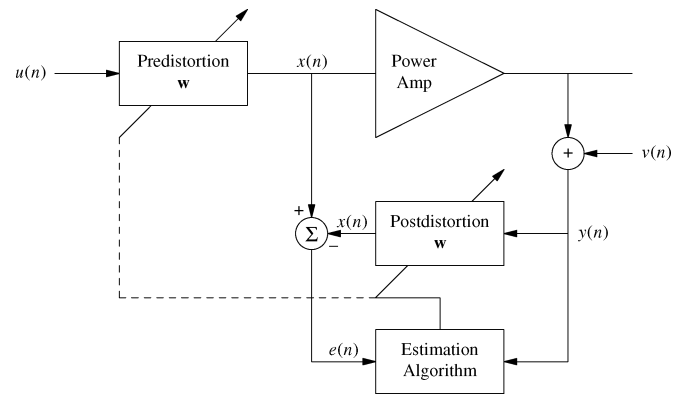

Fig. 3. Predistortion by inverse modeling.

III. Inverse Structures

Having introduced a number of amplifier memory structures, we now go on to apply these to the predistortion problem of Fig. 1. We will discuss two methods for doing this: a general inverse Volterra method and an indirect method that is applicable to any model.

The most straightforward approach is to first estimate the parameters of the nonlinear memory amplifier model and then derive an inverse nonlinear memory predistortion function. Within the general framework of Volterra systems, there is a technique known as the *pth-order inverse* [9] that accomplishes this. The pth-order inverse method has been applied to nonlinear equalization [24] as well as to predistortion of a TWT amplifier used in wavelet packet division multiplexing [25].

The pth-order inverse involves a good deal of computation, which is undesirable for real-time, wideband applications. Fortunately, there is an alternative that reduces the procedure to a one-step problem. The idea, proposed by Eun and Powers [26], is depicted in Fig. 3. Here, an *inverse* amplifier model is identified in the first place by using the output of the amplifier to predict its input. We call this process *postdistortion* because it is applied following the amplifier. Then, the estimated parameters of the inverse model are copied to an identical model that is used to predistort the input. All of this is quite intuitive and appealing. Any of the models discussed in the last section can be used for the inverse model.

There is one small worry about this technique: Will the response of an amplifier followed by postdistortion be the same as the response to the same model applied *before* the amplifier? We are so used to linear systems that such questions about commutability do not ordinarily arise. Fortunately, again thanks to Schetzen, there is a theoretical foundation that justifies this approach. In [9, ch. 7], it is shown that if one has a pth-order postinverse of a general Volterra system, then the pth-order preinverse is identical. Thus, to arbitrary order of approximation, predistortion is equivalent to postdistortion in our application.

IV. Estimation Algorithms

There are a number of least-squares-type algorithms for estimating model coefficients that appear as a linear weighting of nonlinear signals, such as in (23) and (24). The easiest way to

Authorized licensed use limited to: Technion Israel Institute of Technology. Downloaded on November 09,2022 at 15:11:17 UTC from IEEE Xplore. Restrictions apply.

formulate such a problem is to first collect the coefficients, e.g., a_{kl}, b_{klm}, c_{klm} in (23) or (24), into one $J \times 1$ vector, say $\mathbf{w}$, where J is the total number of coefficients. Each component of the coefficient vector $\mathbf{w}$ is associated with a signal whose time samples over some period, say $n = 1, 2, \cdots, N$, are collected into a vector. For example, in (23), coefficient a_{21} is associated with the signal $x(n-1)|x(n-1)|^2$, whose time samples define an $N \times 1$ vector. Assembling all such vectors into a $N \times J$ matrix $\mathbf{X}$, the model output can then be compactly expressed as

$$\hat{\mathbf{y}} = \mathbf{X}\mathbf{w} \tag{25}$$

where $\hat{\mathbf{y}}$ is an $N \times 1$ vector that designates an estimate of the actual output vector $\mathbf{y}$.

For the inverse modeling method used in the predistortion technique of Fig. 3, we have the analogous setup

$$\hat{\mathbf{x}} = \mathbf{Y}\mathbf{w} \tag{26}$$

where now the input is being estimated from the output samples, and so, $\mathbf{Y}$ is constituted similar to $\mathbf{X}$ with $y(n-m)$ replacing $x(n-m)$. This is the actual form of the estimation employed in the context of our predistortion applications.

As in Fig. 3, the estimation error is written

$$e(n) = x(n) - \hat{x}(n) \tag{27}$$

or in vector form over a block of N samples as

$$\mathbf{e} = \mathbf{x} - \hat{\mathbf{x}}. \tag{28}$$

It is now a simple matter to write the least-squares solution that minimizes $\|\mathbf{e}\|^2$ as follows:

$$\mathbf{w} = (\mathbf{Y}^H\mathbf{Y})^{-1}\mathbf{Y}^H\mathbf{x}. \tag{29}$$

Although we formally write the inverse of the $J \times J$ sample covariance matrix $\mathbf{Y}^H\mathbf{Y}$, this will almost always be computed by obtaining $\mathbf{w}$ as the solution of the set of linear equations

$$\mathbf{Y}^H\mathbf{Y}\mathbf{w} = \mathbf{Y}^H\mathbf{x}. \tag{30}$$

For example, in Matlab, the "backslash" ($\backslash$) operator solves equations of the form (30) by Cholesky decomposition and forward/backward substitution. The computational complexity is $O(J^2)/$ sample, where J is the dimensionality, i.e., number of coefficients to be estimated.

Note that measurement noise associated with $y(n)$ will slightly bias the solution, due to the nonlinearity of $\mathbf{Y}$. A discussion of this problem and remedial techniques are presented in [27].

A variant of the algorithm can be used to partially update $\mathbf{w}$ from a previous estimate, thereby forcing some continuity from block to block. This is formulated as a "damped" Newton algorithm

$$\mathbf{w}_{p+1} = \mathbf{w}_p + \mu(\mathbf{Y}^H\mathbf{Y})^{-1}\mathbf{Y}^H\mathbf{e} \tag{31}$$

where p is the block index and μ is the "relaxation" constant. If $\mu = 1$ and $\mathbf{w}_0 = 0$, then the algorithm converges to the least-squares solution (29) in one step. For $\mu < 1$, there is some memory introduced that constrains how much $\mathbf{w}$ can change from one block to the next. This form also has the advantage of robustness in that the error $\mathbf{e}$ drives the weight update, and so always obtains a solution that minimizes the average error.

In many applications, adaptive estimation is much more efficiently performed on a sample-by-sample basis, which minimizes storage requirements and, like the above, also enjoys the benefits of error feedback. Stochastic gradient algorithms like the so-called *least mean-square* (LMS) algorithm [28] are particularly efficient, having $O(J)/$sample complexity. However, for the predistortion application, the higher order nonlinearities are always small, thereby resulting in a poorly conditioned covariance matrix. In this case, stochastic gradient algorithms will experience extremely slow convergence and are therefore not practical for this application.

Other sample-by-sample adaptive estimation algorithms are available that converge fast and are not adversely affected by the covariance matrix conditioning. The most popular of these is the *recursive least-squares* (RLS) algorithm [28], which updates the inverse covariance matrix with each new sample and forms a Kalman-like coefficient update. However, RLS is much more computationally intensive, being roughly $O(J^2)/$sample, just like conventional batch solutions of (30). Computationally fast versions are available, but these, like LMS, suffer from poorly conditioned covariance matrices and are prone to instability and divergence. Moreover, the storage advantage of sample-by-sample algorithms is largely obviated for most predistortion applications because high-speed samples must be collected in batches anyway; it is not currently feasible to do such computations on the fly for wideband communication signals.

In [29] and references therein, data-adaptive, or sample-by-sample, versions of the conjugate gradient (CG) algorithm are discussed for adaptive filtering applications. These are similar in spirit to stochastic gradient algorithms like LMS, but potentially enjoy faster convergence like RLS. In fact, it is generally acknowledged that the performance is comparable to RLS, so the only issue is whether any computational advantage can be gained. Unless matrix-vector multiplications can be avoided, there will not be any advantage of stochastic CG over RLS. The only way to avoid this is to use recursive updating of the residual vector [29, eq. (20)] over a sliding window of M samples. This will offer a computational advantage only if M is smaller than the number of coefficients, or dimension, J. However, a well-known rule of thumb (originally propounded many years ago by Reed, Mallett, and Brennan [30] in the context of adaptive arrays) states that to achieve performance degradation of less than 3 dB, one needs to use approximately $2J$ vector samples to estimate the covariance matrix. The stochastic CG case is a little different since we are only using the M vector samples to estimate the residual directions. Nevertheless, the analysis and

Authorized licensed use limited to: Technion Israel Institute of Technology. Downloaded on November 09,2022 at 15:11:17 UTC from IEEE Xplore. Restrictions apply.

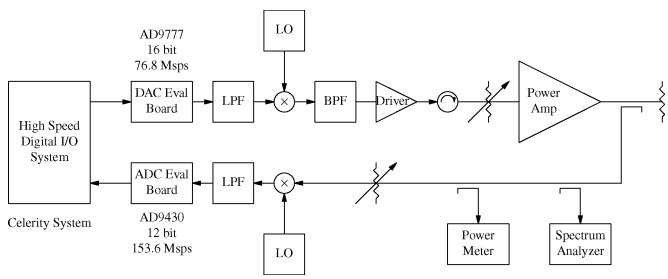

Fig. 4. Block diagram of experimental testbed.

simulations in [29, Tables II and VI] seem to reinforce this requirement. Our intuition is that with stochastic CG, if you do not get a direction quite right, the minimum error will be compromised. Also worthwhile mentioning is the observation in [29] that it is important to periodically reset the direction vector to the true gradient in order to ensure convergence.

Thus, for all of the above reasons, we favor least-squares-type batch solutions for estimating model coefficients.

V. Experimental Results

A. Description of Experimental Testbed

Fig. 4 shows a block diagram of the experimental testbed. The analog hardware starts at the data converters. On the transmit side, an Analog Devices AD9777 digital-to-analog converter (DAC) uses both I and Q digital ports simultaneously. The DAC is supplied with a 307.2-MHz continuous-wave (CW) sampling clock from the SYN400 card in a Celerity digital I/O storage system, and the 76.8-MHz signal data is then internally interpolated in the DAC to the 307.2-MHz rate. In addition, the DAC centers the output analog IF signal at $f_s/4$ (also 76.8 MHz).

The linearity of the signal at the DAC output is about a 63-dB adjacent channel power (ACP) ratio for a three-carrier UMTS signal. The signal is then lowpass-filtered and passively mixed through a ZLW-11H Mini-Circuits double-balanced mixer up to the PCS or UMTS RF band (1930–1990 MHz or 2110–2170 MHz). The local oscillators (LOs) for the transmitter as well as the receiver are standalone A3640A Agilent synthesized signal generators. After being upconverted, the signal is then padded and RF bandpass filtered to reduce the local oscillator (LO) leakage. The signal is then put through a highly linear SM1720-44L Stealth Microwave 20-W driver amplifier, which maintains the signal linearity to about 59-dB ACP. After an isolator and some variable attenuators, the signal is then applied to the amplifier under test.

The signal acquires distortion in the power amplifier and the output is fed into a coupling network which allows monitoring of the signal by a spectrum analyzer and power meter, as well as dumping most of the power into a high-power load. The coupled output signal is also returned to the receiver through a variable attenuator bank.

The receiver is comprised of a high-linearity Watkins-Johnson WJ-HMJ7 mixer and IF lowpass filter. The signal then proceeds to an Analog Devices AD9430 analog-to-digital converter (ADC), sampled at 153.6 MHz from a standalone phase-locked-loop voltage-controlled oscillator (VCO). The signal integrity at this point (analog domain) is approximately 59–60-dB ACP when the amplifier under test is removed from the loop. The ADC then sends the separate digital I and Q signals back to the Celerity box, where the data gets dumped to the memory boards and then accessed by Matlab software running the predistortion algorithms.

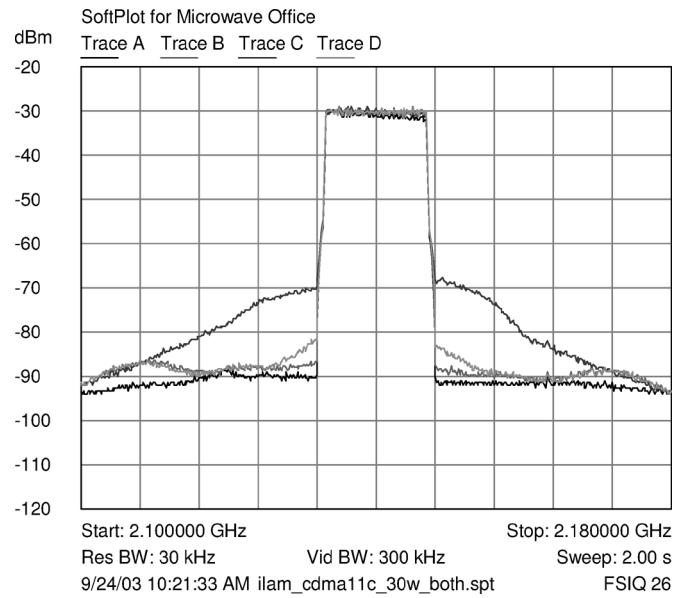

Fig. 5. Experimental power spectra. From top to bottom: No predistortion, memory polynomial, generalized memory polynomial, input signal.

All the data converter clocks and RF VCOs are locked to a global 10-MHz source from the Celerity box.

B. Procedure

In the experiments of this paper, we used an IMT (International Mobile Telecommunications) band linear amplifier module (ILAM) power amplifier supplied by the Andrew Corporation. The amplifier was operated at 2.14 GHz with an output power of 30 W. The input signal used for the experiments reported here was an 11-carrier CDMA signal with a total bandwidth of approximately 15 MHz. All signal processing was done offline by using the Celerity to capture a block of 40 000 samples, using Matlab routines to estimate the predistorter parameters, and again using the Celerity to output a continuous stream of data with a periodic repetition of a 500 000-sample output block (with filtering to smooth over the discontinuity from head to tail). Since the input spectrum to the amplifier is affected by the predistorter (the "Predistortion" box in Fig. 3), which is copied from the previous coefficient estimates (the "Postdistortion" box in Fig. 3), several estimation iterations are necessary. However, convergence is fast and there is not much change after two iterations. We used three to four iterations for most of the tests reported here. Analog spectra were measured using an FSIQ26 Rohdes & Schwarz signal analyzer with 2-s averaging time.

C. Results

A power spectrum of the amplifier analog input is shown by the lowest trace in in Fig. 5, which demonstrates over 60 dB of

Authorized licensed use limited to: Technion Israel Institute of Technology. Downloaded on November 09,2022 at 15:11:17 UTC from IEEE Xplore. Restrictions apply.

TABLE I
EXPERIMENTAL MEASUREMENTS

Nbr Coeffs.	$\mathcal{K}_a$	$\mathcal{L}_a$	$\mathcal{K}_b$	$\mathcal{L}_b$	$\mathcal{M}_b$	$\mathcal{K}_c$	$\mathcal{L}_c$	$\mathcal{M}_c$	MSE	ACP				Nbr Iter.
										–2	–1	+1	+2	
20	[0:4]	[0:3]	[]	[]	[]	[]	[]	[]	–33.33	–57.11	–52.48	–53.07	–57.89	3
30	[0:4]	[0:5]	[]	[]	[]	[]	[]	[]	–33.66	–57.72	–53.01	–53.55	–58.17	5
40	[0:4]	[0:7]	[]	[]	[]	[]	[]	[]	–34.61	–57.30	–52.92	–54.04	–57.90	4
30	[0:4]	[0:1]	[2 4]	0	[1:10]	[]	[]	[]	–33.14	–58.13	–55.35	–56.01	–57.68	3
40	[0:4]	[0:3]	[2 4]	0	[1:10]	[]	[]	[]	–33.86	–58.59	–56.46	–56.96	–58.32	3
50	[0:4]	[0:5]	[2 4]	0	[1:10]	[]	[]	[]	–34.84	–57.99	–57.06	–56.79	–58.78	7
60	[0:4]	[0:7]	[2 4]	0	[1:10]	[]	[]	[]	–34.95	–57.70	–56.72	–56.84	–57.61	3
26	[0:4]	[0:3]	[2 4]	0	[1:3]	[]	[]	[]	–33.99	–58.07	–56.68	–57.00	–58.85	3
32	[0:4]	[0:3]	[1:4]	0	[1:3]	[]	[]	[]	–33.96	–58.83	–56.76	–56.89	–58.81	4
68	[0:4]	[0:3]	[1:4]	[0:3]	[1:3]	[]	[]	[]	–33.86	–58.09	–57.60	–56.20	–58.81	4
44	[0:4]	[0:3]	[2 4]	[0:3]	[1:3]	[]	[]	[]	–33.49	–58.33	–56.80	–56.87	–58.35	6
40	[0:4]	[0:3]	[2 4]	0	[1:5]	[2 4]	0	[1:5]	–34.79	–57.61	–56.80	–56.23	–57.93	4

dynamic range. The highest trace shows the spectral regrowth of the amplifier output without predistortion and is seen to be as high as -40 dB relative to the in-band level. The next trace down shows the output spectrum with the memory polynomial model of Section II-D with nonlinearity order $K = 5$ and $M = 4$ delay taps (20 coefficients total). This is seen to bring down the spectral regrowth to less than about -52 dB. The next trace is for the generalized memory polynomial model of Section II-G using the same coefficient order for the memory polynomial part ($K_a = 5$, $L_a = 4$), and with the addition of lagging envelope cross-terms of order $\mathcal{K}_b = [2, 4]$ and $L_b = 10$ taps (40 coefficients total). The cross terms are seen to further reduce the regrowth to about the -59-dB level.

The measured results for the above as well as other coefficient orders are listed in Table I. The first column is the total number of coefficients. The next two columns are the coefficient index arrays $\mathcal{K}_a$ and $\mathcal{L}_a$ corresponding to the memory polynomial part of the generalized polynomial model (24). The next three columns correspond to the index arrays $\mathcal{K}_b$, $\mathcal{L}_b$, and $\mathcal{M}_b$ for signal and lagging envelope cross terms, followed next by $\mathcal{K}_c$, $\mathcal{L}_c$, and $\mathcal{M}_c$ for signal and leading envelope cross terms. The mean-square error (MSE) associated with the coefficient estimation (26)–(29) appears in the next column. The next four columns are the ACP ratios measured, respectively, in the two lower and two upper adjacent channel slots, which are spaced at contiguous 15-MHz intervals. Finally, the last column shows the number of iterations used in estimation.

As can be seen, the ACP is generally reduced as the coefficient order is increased. However, some coefficients are more efficient than others in achieving a given ACP level. As the model order increases, the ACP is seen to bottom out at about the -59-dB level. Currently, the ACP limitation is due to the noise floor of the DAC used in the testbed.

VI. CONCLUSION

In this paper, the search for wideband predistortion models culminated in the generalized memory polynomial, which combines the memory polynomial with cross terms between the signal and lagging and/or leading exponentiated envelope terms. The cross terms significantly improve the performance in reducing the ACP level, achieving the best results to date. However, meaningful comparisons of the effectiveness of various parameter sets is difficult once the DAC noise floor has been reached. What we can say at present is that ACP of -58 dB is attainable for 15-MHz signals, and this is more than adequate to meet most spurious emission requirements, with some margin to spare. Development of theoretical models to better understand the nature of amplifier distortion and memory effects is also hampered at present by the noise floor problem. A better theoretical characterization would enable theoretical performance analysis of actual power amplifier behavior. Thus, future research awaits the development of better experimental hardware components. In the way of practical product development, it would be useful to perform extensive testing regarding the effects of temperature variations, power levels, etc., to assure compliance with system requirements.

REFERENCES

[1] P. B. Kenington, *High-Linearity RF Amplifier Design*. Boston, MA: Artech House, 2000.
[2] ——, "Linearized transmitters: An enabling technology for software defined radio," *IEEE Commun. Mag.*, vol. 40, pp. 156–162, Feb. 2002.
[3] A. A. M. Saleh and J. Salz, "Adaptive linearization of power amplifiers in digital radio systems," *Bell Syst. Tech. J.*, vol. 62, pp. 1019–1033, Apr. 1983.
[4] J. K. Cavers, "Amplifier linearization using a digital predistorter with fast adaptation and low memory requirements," *IEEE Trans. Veh. Technol.*, vol. 39, pp. 374–382, Nov. 1990.
[5] A. N. D'Andrea, V. Lottici, and R. Reggiannini, "Nonlinear predistortion of OFDM signals over frequency-selective fading channels," *IEEE Trans. Commun.*, vol. 49, pp. 837–843, May 2001.
[6] W. Bösch and G. Gatti, "Measurement and simulation of memory effects in predistortion linearizers," *IEEE Trans. Microw. Theory Tech.*, vol. 37, pp. 1885–1890, Dec. 1989.
[7] J. F. Sevic, K. L. Burger, and M. B. Steer, "A novel envelope-termination load-pull method for ACPR optimization of RF/microwave power amplifiers," in *Proc. Microwave Symp. Dig.*, 1998, pp. 723–726.
[8] J. Lajoinie, E. Ngoya, D. Barataud, J. M. Nebus, J. Sombrin, and B. Rivierre, "Efficient simulation of NPR for the optimum design of satellite transponders SSPAs," in *Proc. Microwave Symp. Dig.*, 1998, pp. 741–744.
[9] M. Schetzen, *The Volterra and Wiener Theories of Nonlinear Systems*. New York: Wiley, 1980.
[10] G. M. Raz and B. D. Van Veen, "Baseband Volterra filters for implementing carrier based nonlinearities," *IEEE Trans. Signal Process.*, vol. 46, no. 1, pp. 103–113, Jan. 1998.
[11] C.-H. Cheng and E. J. Powers, "Optimal Volterra kernel estimation algorithms for a nonlinear communication system for PSK and QAM inputs," *IEEE. Trans. Signal Process.*, vol. 49, no. 1, pp. 147–163, Jan. 2001.
[12] H. W. Kang, Y. S. Cho, and D. H. Youn, "Adaptive precompensation of Wiener systems," *IEEE Trans. Signal Process.*, vol. 46, no. 10, pp. 2825–2829, Oct. 1998.

Authorized licensed use limited to: Technion Israel Institute of Technology. Downloaded on November 09,2022 at 15:11:17 UTC from IEEE Xplore. Restrictions apply.

[13] ——, "On compensating nonlinear distortions of an OFDM system using an efficient adaptive predistorter," *IEEE Trans. Commun.*, vol. 47, no. 4, pp. 522–526, Apr. 1999.
[14] P. Celka, N. J. Bershad, and J.-M. Vesin, "Stochastic gradient identification of polynomial Wiener systems: analysis and application," *IEEE Trans. Signal Process.*, vol. 49, no. 2, pp. 301–313, Feb. 2001.
[15] A. E. Nordsjö and L. H. Zetterberg, "Identification of certain time-varying nonlinear Wiener and Hammerstein systems," *IEEE Trans. Signal Process.*, vol. 49, no. 3, pp. 577–592, Mar. 2001.
[16] N. J. Bershad, P. Celka, and S. McLaughlin, "Analysis of stochastic gradient identification of Wiener–Hammerstein systems for nonlinearities with Hermite polynomial expansions," *IEEE Trans. Signal Process.*, vol. 49, no. 5, pp. 1060–1072, May 2001.
[17] J. Kim and K. Konstantinou, "Digital predistortion of wideband signals based on power amplifier model with memory," *Electron. Lett.*, vol. 37, pp. 1417–1418, Nov. 2001.
[18] L. Ding, G. T. Zhou, D. R. Morgan, Z. Ma, J. S. Kenney, J. Kim, and C. R. Giardina, "A robust digital baseband predistorter constructed using memory polynomials," *IEEE Trans. Commun.*, vol. 52, no. 1, pp. 159–165, Jan. 2004.
[19] H. Ku, M. D. Mckinley, and J. S. Kenney, "Extraction of accurate behavior models for power amplifiers with memory effects using two-tone measurements," in *Proc. IEEE MTT-S Int. Microwave Symp. Dig.*, 2002, vol. 1, pp. 139–142.
[20] M. Schetzen, "Nonlinear system modeling based on the Wiener theory," *Proc. IEEE*, vol. 69, pp. 1557–1573, Dec. 1981.
[21] Z. Ma, M. Zierdt, and J. Pastalan, "Characterization of power amplifier memory effect for digital baseband predistortion," unpublished.
[22] L. Ding, Z. Ma, D. R. Morgan, and M. Zierdt, "A least-squares/Newton method for digital predistortion of wideband signals," *IEEE Trans. Commun.*, vol. 54, no. 5, pp. 833–840, May 2006.
[23] A. Zhu, "Behavioral modeling of RF power amplifiers based on pruned Volterra series," *IEEE Microw. Wireless Compon. Lett.*, vol. 14, pp. 563–565, Dec. 2004.
[24] Y.-W. Fang, L.-C. Jiao, X.-D. Zhang, and J. Pan, "On the convergence of Volterra filter equalizers using a Pth-order inverse approach," *IEEE Trans. Signal Process.*, vol. 49, no. 8, pp. 1734–1744, Aug. 2001.
[25] K.-F. To, P. C. Ching, and K. M. Wong, "Compensation of amplifier nonlinearities on wavelet packet division multiplexing," in *Proc. IEEE Int. Conf. Acoustics, Speech, Signal Processing*, 2001, pp. 2669–2672.
[26] C. Eun and E. J. Powers, "A new Volterra predistorter based on the indirect learning architecture," *IEEE Trans. Signal Process.*, vol. 45, no. 1, pp. 223–227, Jan. 1997.
[27] D. R. Morgan, Z. Ma, and L. Ding, "Reducing measurement noise effects in digital predistortion of RF power amplifiers," in *Proc. Int. Conf. Communications (ICC)*, 2003, pp. 2436–2439.
[28] S. Haykin, *Adaptive Filter Theory*. Englewood Cliffs, NJ: Prentice-Hall, 1991.
[29] P. S. Chang and A. N. Willson, Jr., "Analysis of conjugate gradient algorithms for adaptive filtering," *IEEE Trans. Signal Process.*, vol. 48, no. 2, pp. 409–418, Feb. 2000.
[30] I. S. Reed, J. D. Mallett, and L. E. Brennan, "Rapid convergence rate in adaptive arrays," *IEEE Trans. Aerosp. Electron. Syst.*, vol. AES-10, pp. 853–863, Nov. 1974.

Dennis R. Morgan (S'63–S'68–M'69–SM'92) was born in Cincinnati, OH, on February 19, 1942. He received the B.S. degree from the University of Cincinnati, OH, in 1965 and the M.S. and Ph.D. degrees from Syracuse University, Syracuse, NY, in 1968 and 1970, respectively, all in electrical engineering.

From 1965 to 1984, he was with the Electronics Laboratory, General Electric Company, Syracuse, NY, specializing in the analysis and design of signal processing systems used in radar, sonar, and communications. He is currently a Distinguished Member of Technical Staff with Bell Laboratories, Lucent Technologies, Murray Hill, NJ, where he has been employed since 1984: from 1984 to 1990, he was with the Special Systems Analysis Department, Whippany NJ, where he was involved in the analysis and development of advanced signal processing techniques associated with communications, array processing, detection and estimation, and active noise control; from 1990 to 2002, he was with the Acoustics Research Department, Murray Hill, NJ, where he was engaged in research on adaptive signal processing techniques applied to electroacoustic systems, including adaptive microphones, echo cancellation, talker direction finders, and blind source separation; since 2002, he has been with the Wireless Research Laboratory, Murray Hill NJ, where he is involved in research on adaptive signal processing applied to radio frequency and optical communication systems. He has authored numerous journal publications and is coauthor of *Active Noise Control Systems: Algorithms and DSP Implementations* (New York: Wiley, 1996) and *Advances in Network and Acoustic Echo Cancellation* (New York: Springer-Verlag, 2001).

Dr. Morgan served as Associate Editor for the IEEE TRANSACTIONS ON SPEECH AND AUDIO PROCESSING from 1995 to 2000 and Associate Editor for the IEEE TRANSACTIONS ON SIGNAL PROCESSING from 2001 to 2004.

Zhengxiang Ma received the B.S. degree in physics from the University of Science and Technology, Hefei, China, in 1989 and the M.S. and Ph.D. degrees in applied physics from Stanford University, Stanford, CA, in 1991 and 1995, respectively.

He joined Bell Laboratories, Lucent Technologies, in 1995, where he is currently a Distinguished Member of Technical Staff in the Wireless and Broadband Access Center, Murray Hill, NJ. His research interests include novel digital signal processing in high-performance base-station radio, power amplifier linearization, and wireless networking infrastructure architecture. He has coauthored several technical papers and holds nine patents.

Jaehyeong Kim received the B.S.E.E. and M.S.E.E. degrees from Seoul National University, Seoul, Korea, in 1988 and 1990, respectively, and the Ph.D. degree in electrical engineering from the University of California, Los Angeles, in 1996.

From 1996 to 2004, he was with the Wireless Advanced Technology Laboratory, Lucent Technologies. He joined Posdata in 2004, and has been working in the area of WiMAX/WiBro system development. His interests are in channel coding and modulation, signal processing for communication systems, power amplifier predistortion, and architectures for upcoming wireless communication systems.

Mike G. Zierdt was born in Queens, NY, in December 1965. He received the B.S.E.E. and M.S.E.E. degrees from Polytechnic University, Brooklyn, NY, in 1988 and 1994.

For four years, he worked at Mini Circuits Laboratories as an RF components designer, followed by six years in the Consumer Products Division of AT&T/Lucent Technologies, working primarily on wireless handsets. For the past seven years, he has been in the Wireless Research Laboratory in Bell Laboratories, Murray Hill, NJ, working on a variety of transceivers and RF components.

John Pastalan was born in Binghamton, NY. He received the B.S. degree in physics and the M.S. degree in applied physics from the State University of New York at Binghamton in 1986 and 1989, respectively.

He is currently a Member of Technical Staff in the Wireless Access Systems Department of Bell Laboratories, Lucent Technologies, Murray Hill, NJ.

Authorized licensed use limited to: Technion Israel Institute of Technology. Downloaded on November 09,2022 at 15:11:17 UTC from IEEE Xplore. Restrictions apply.